



Energy, Mines and  
Resources Canada

Énergie, Mines et  
Ressources Canada

580434

Earth Physics Branch

Direction de la physique du globe

1 Observatory Crescent  
Ottawa Canada  
K1A 0Y3

1 Place de l'Observatoire  
Ottawa Canada  
K1A 0Y3

**Geothermal Service  
of Canada**

**Service géothermique  
du Canada**

THE ACOUSTIC PROPERTIES OF METHANE HYDRATE

BY BRILLOUIN SPECTROSCOPY

- PRELIMINARY REPORT

M.J. Clouter and H. Kiefte  
Department of Physics,  
Memorial University of Newfoundland

Earth Physics Branch Open File Number 79-18

Ottawa, Canada 1979

i + 14 pp. including 4 figures.

Price \$10.00

NOT FOR REPRODUCTION

EPB  
Open File  
79-18

This document was produced  
by scanning the original publication.

Ce document est le produit d'une  
numérisation par balayage  
de la publication originale.



Energy, Mines and  
Resources Canada

Énergie, Mines et  
Ressources Canada

Earth Physics Branch

Direction de la physique du globe

---

1 Observatory Crescent  
Ottawa Canada  
K1A 0Y3

1 Place de l'Observatoire  
Ottawa Canada  
K1A 0Y3

**Geothermal Service  
of Canada**

**Service géothermique  
du Canada**

THE ACOUSTIC PROPERTIES OF METHANE HYDRATE

BY BRILLOUIN SPECTROSCOPY

- PRELIMINARY REPORT

M.J. Clouter and H. Kiefte  
Department of Physics,  
Memorial University of Newfoundland

Earth Physics Branch Open File Number 79-18

Ottawa, Canada 1979

i + 14 pp. including 4 figures.

Price \$10.00

NOT FOR REPRODUCTION

## Abstract

Under certain conditions of pressure and temperature hydrocarbon gases combine with water to form an ice-like solid, methane hydrate . Such conditions are encountered in the permafrost areas of Canada and beneath the offshore waters surrounding us. Very little information on the physical properties of hydrates is currently available although such data is needed to evaluate and assess natural hydrate deposits. This preliminary report describes the formation of methane hydrate in the laboratory and the experimental equipment to be used in determining the acoustic properties of single crystals of hydrate.

## Résumé

Sous certaines conditions de pression et de température le gaz naturel et l'eau se combinent pour former une substance semblable à la glace, les hydrates de méthane. Au Canada nous rencontrons de telles conditions dans les zones de pergélisol et sous les mers qui nous côtoient. Présentement, très peu de données sur les propriétés physiques des hydrates sont disponibles, quoique cette information est nécessaire à l'évaluation des dépôts naturels d'hydrates. Dans ce rapport préliminaire la formation, en laboratoire, des hydrates de méthane est décrite de même que l'équipement qui sera utilisé pour déterminer les propriétés acoustiques d'un cristal unique d'hydrate.

THE ACOUSTIC PROPERTIES OF METHANE HYDRATE  
BY  
BRILLOUIN SPECTROSCOPY

A Report  
by  
M. J. Clouter and H. Kiefte  
Department of Physics  
Memorial University of Newfoundland  
St. John's, Newfoundland, A1B3X7

Re: DSS File Number 05SU.23235-9-0485; Serial Number 0SU79-00052

## INTRODUCTION

The application of seismic techniques to the detection of methane hydrate in the natural environment requires a knowledge of the acoustic velocities in a material whose mode of occurrence, e.g. whether in essentially pure form or as a sediment/hydrate mixture, is largely unknown. It is clear, however, that in the absence of other information a knowledge of the acoustic properties of the pure hydrate may be of considerable value. Although relevant theoretical estimates have been made by Whalley (1979), no experimental data of this kind are available. It is consequently the purpose of the present work to determine acoustic velocities in pure methane hydrate via the method of Brillouin spectroscopy.

Methane Hydrate.

The pure gas hydrates are crystalline, ice-like substances belonging to a class of inclusion compounds called clathrates. The gas molecules, usually referred to as guest molecules, are effectively trapped without the normal chemical bonding in cavities of dodecahedral geometry which are formed in the structure of the host material (water). Under conditions of gas saturation the result is a stable crystalline material whose structural characteristics have been determined for a fairly large number of different guest molecules (Stoll *et al* 1971 ; Miller 1974).

Depending on the size of the guest molecule, two types of hydrate are possible. For methane, a small hydrating molecule, 8 cavities are available for every 46 water molecules, and this is referred to as structure I (our exclusive concern in the present investigation). Hence as much as one molecule of methane for every 5.75 molecules of water can be trapped in the cage-like structure of the hydrate under appropriate conditions of temperature and pressure (Kaplan 1974 ; Davidson 1973).

The hydrate of methane is unfortunately one of the more difficult ones to produce artificially, largely because of the relatively high pressures involved. Nevertheless several groups have had success via

the method of bubbling pressurized methane through sediment/water mixtures (Stoll et al 1971; Makogan and Sarkis'yants 1976) and crushed ice (Davidson 1979). Such methods are, however, not suitable for optical studies since the samples produced are inevitably cloudy in appearance and would generate a very high intensity of undesired (parasitic) scattering from an incident laser beam. In addition, it is also important to obtain a well defined, preferably cylindrical, geometry for the sample in order to have clear knowledge of the incident and scattered beam directions. It was consequently considered necessary to develop a new technique for forming the methane hydrate samples in the present work.

### Brillouin Spectroscopy

Brillouin spectroscopy is a relatively new experimental technique whose development has paralleled that of the laser and which, in the last few years, has achieved a high level of technical sophistication. It involves the scattering of light due to fluctuations in the dielectric constant which are associated with the thermal noise in fluids and solids. Because of the requirement for simultaneous energy and momentum conservation in the scattering process one, in effect, detects well defined, plane wave, Fourier components of the thermal noise whose frequencies correspond to the hypersonic ( $\sim 10$  GHz) range. The propagation velocity for a given plane (elastic, or sound,) wave is manifested as a Doppler shift in the frequency of the scattered radiation, and the classical theory of the Doppler Effect can be used to advantage in predicting the essential features of the resulting spectrum (see Fig. 1). Brillouin (1914;1922) showed that monochromatic light of wavelength  $\lambda_0$  and frequency  $\nu_0$  can interact strongly with those acoustic waves (wavelength  $\Lambda$ , frequency  $\nu_s$ ) which satisfy the Bragg reflection condition

$$\lambda_0 = 2n\Lambda \sin(\alpha/2) ,$$

thus giving rise to light scattering at a specific angle  $\alpha$ . The above relation can be rewritten as

$$\nu_s = 2\nu_0 (v/c) n \sin(\alpha/2)$$

where  $v$  is the velocity of the acoustic wave,  $c$  is the velocity of light in vacuum, and  $n$  is the refractive index of the medium. Since the Bragg condition is satisfied equally well for velocities  $\pm v$ , the associated Doppler shifts give rise to a Brillouin doublet with frequencies  $\nu_0 \pm \nu_s$ , and this is what is normally observed in liquids and gases. In the case of crystals, however, three sets of Brillouin doublets generally occur, one due to longitudinal acoustic waves and two due to transverse waves, with frequency shifts (i.e. velocities) which depend on crystal orientation. Thus, given that the scattering angle  $\alpha$  is accurately defined by the geometry of the experiment, and given that the refractive index of the medium is known at the wavelength  $\lambda_0$ , then measurement of the frequency shifts leads to a direct determination of the longitudinal and transverse sound velocities. When these velocities are determined as a function of orientation for a single crystal, the elastic constants may be calculated (Stoicheff 1977), and experiments of this kind have been carried out in this laboratory with single crystals of  $\gamma$ -O<sub>2</sub>,  $\beta$ -N<sub>2</sub>,  $\beta$ -CO, and ice Ih (Kieft and Clouter 1975,1976; Gammon *et al* 1979,1980). Similar studies with naturally occurring samples such as glacial, fresh water, and sea ice are in progress.

The principal advantage of Brillouin spectroscopy over the more conventional ultrasonic methods is that the elastic waves being probed are not artificially excited. Perturbation of the sample is consequently minimized and problems associated with the bonding of transducers to the sample are eliminated. In addition, the sample size can be greatly reduced (as small as 1 mm<sup>3</sup>) so that the technique is particularly suitable for the relatively high pressures required in the methane hydrate investigations.

#### APPARATUS

The overall arrangement of the apparatus is shown schematically in Fig. 2. The incident light is provided by a single mode argon-ion laser (Spectra Physics model 165-08). X-rays are used in these experiments to monitor crystal quality and for determination of crystal

orientation by Laue diffraction.

### Fabry-Perot Spectrometer

The scattered light is analyzed using a piezoelectrically scanned, triple pass Fabry-Perot interferometer (Burleigh Instruments Inc.) and detected with a cooled photomultiplier tube (ITT FW130). The output from the photomultiplier is coupled through an amplifier-discriminator (Princeton Applied Research model 1120) to a data acquisition and control system (Burleigh model DAS-1) which also provided the repetitive ramp voltage used in scanning the interferometer. The multichannel analyzer of the DAS system accumulated spectral data in the form of photon counts (intensity) versus channel number, the latter being proportional to the Fabry-Perot mirror separation and hence to the frequency of the scattered light. Additionally, the DAS system utilizes negative feedback circuitry to compensate for drifts in frequency associated with thermal and mechanical effects throughout the system, thereby permitting arbitrarily long spectral accumulation times.

### Sample Cell and Cryostat

A schematic diagram of the sample cell and cryostat is shown in Fig. 3. The basic consideration in the design of this unit was to make it as simple and effective as possible (see also Ahmad et al 1978; Gammon et al 1980).

The sample cell consisted of a quartz tube of 1 mm inner diameter and 6 mm outer diameter. In the normal light scattering experiment the lower end of the cell is closed with a high quality cylindrical quartz window, but in the preliminary experiments which concentrated on the hydrate formation process this closure was accomplished by fusion of the tube. As shown in Fig. 4 the top end of the quartz tube was flared and ground to provide a pressure seal to the gas handling system. With reference to Fig. 3, a spring clip made of brass shim and about 5 mm wide was fastened to the bottom of the cell with a screw mounted GaAs diode attached. One junction of a differential copper-constantan thermocouple was also mounted near the diode using a thermal epoxy. Another clip was attached to the cell at a height of about 1 cm above the first clip and the second thermocouple junction was fastened to it.



Small copper rods were soldered to each clip, and conduction paths to a thermoelectric cooling element were provided by flexible copper braids which were soldered to the rods and pressure-bonded to the cold surface of the thermoelectric module. The hot surface of the module was thermally anchored to a copper heat sink which was cooled by a continuous and constant flow of cold water. The associated 0-6 VDC power supply provided currents up to 6 A and temperatures down to  $-20^{\circ}\text{C}$  could be maintained at the top clip. The temperature of the sample was both monitored and controlled via a Lakeshore Cryotronics Indicator/Controller model DTC500 which was used in conjunction with the GaAs diode thermometer and two  $50\ \Omega$  heaters wound on the copper rods mentioned above.

The entire cell assembly and cooling module were enclosed in a plexiglas tube of 8.8 cm inner diameter and 9.4 cm outer diameter, the sample cell being suspended along the (vertical) axis of the tube. The top and bottom of the cryostat were closed with plexiglas covers 1.3 cm thick which incorporated rubber o-ring seals to assure leak free performance under vacuum. Similar seals were used to mount a polished quartz window at the centre of the bottom cover and to provide a feedthrough for the coolant water: the top cover contained a pumping port and electrical feedthroughs. It was necessary to evacuate the cryostat in order to prevent condensation of water vapor on the outside of the sample cell, and also to provide adequate thermal insulation if the lowest temperatures were desired.

#### Gas Handling System

The most recent version of the high pressure gas handling system is shown in Fig. 4. The pressure is controlled by a regulator at the supply bottle and an adjustable (0-1000 psi) relief valve which vented the gas to atmosphere when a continuous flow was required. The flow rate is controlled by a small orifice metering valve and monitored via the bubble rate through an open container of water. Copper tubing of  $\frac{1}{4}$  inch diameter was used throughout the system, while the high pressure water 'bomb' was constructed of heavy brass and was pretested to 2500 psi. When desired, the gas flow was directed to the sample site via a stainless steel (hypodermic) tube of 0.4 mm inner diameter and 0.7 mm

outer diameter, and flow rates as low as a few  $\text{cm}^3$  per hr (at STP) could be reliably maintained. A 1000 psi rupture disc was installed in the system for safety reasons.

#### SAMPLE PREPARATION

Essentially three different methods were employed to form samples of methane hydrate, and each will be discussed separately.

##### Method 1

The initial approach involved a somewhat simpler version of the gas handling system than that shown in Fig. 4, in that no provision was made for gas flow: the relief valve, metering valve, and hypodermic tube were not included. Before the methane gas was admitted to the system an ice crystal was first formed and grown to fill the sample region to a height of about 3 mm above the top clip. This was accomplished by first evacuating the system and then allowing water vapor to condense into the cell from the reservoir. In order to promote nucleation of the hydrate the top of the ice crystal was formed to a sharp point by the process of pumping on it for about an hour. The temperature of this tip was then brought to about  $-5^\circ\text{C}$  and the system was pressurized (statically) with methane gas. Since the formation pressure for methane hydrate at  $0^\circ\text{C}$  is slightly less than 400 psi (Hand et al 1974; Makogan and Sarkis'yant 1976), these experiments were performed in the 400-700 psi range and it was expected that water vapor would diffuse from the reservoir into the cell to result in a slow but continual formation of hydrate on the ice tip. It became apparent, however, that the diffusion rate for water vapor through the high pressure methane was far short of being sufficient for this purpose. Methane hydrate was nevertheless produced, particularly at the higher pressures, but mainly through direct inclusion of methane into the surface at the ice tip. This process generally took several days and the presence of hydrate was inferred from the observation that when the ice tip was melted a thin conical shell remained intact until the methane pressure was reduced below the hydrate dissociation pressure at the particular temperatures involved. Breakdown of the hydrate was accompanied by the collapse of the conical shell into the water, and the subsequent release of gas bubbles for a

surprisingly long period of time ( $\frac{1}{2}$  hr or more).

### Method 2

Clearly, one of the problems in Method 1 was an insufficient supply of water vapor in the hydrate formation region. The system was therefore modified (Fig.4) to permit a continuous flow of methane through the water in the high pressure reservoir and then into the cell, thereby providing a continuous supply of water-saturated methane gas in the hydrate formation region. The ice crystal was maintained as in Method 1 and the space for forming the hydrate (between the ice and the tip of the hypodermic tube) was from 2 to 3 mm in length. With this approach it was soon found that if any part of the hydrate formation region, or the tip of the hypodermic tube, was above the hydrate formation temperature at the methane pressure used, then liquid water would readily condense. It was, of course, not difficult to produce such conditions since any gas flow is accompanied by a heat flow into this region. Consequently, it was necessary to reduce the temperature at the top of the ice from  $-5^{\circ}\text{C}$  to  $-20^{\circ}\text{C}$ , and methane pressures near 700 psi were used. Hydrate was then produced for a range of methane flow rates.

For the slowest flow conditions (a few  $\text{cm}^3$  per hr at STP) the hydrate favored forming along the cell walls above the ice (rather than forming and growing on top of the ice), even after presaturation for a day with methane gas. So again only a thin, cloudy shell of hydrate was produced. However, with the faster flow rates it was possible to produce a bulk sample ( $\sim 1 \text{ mm}^3$ ) which blocked the quartz tube about halfway between the ice surface and the hypodermic tip. Formation along the cell walls was also observed at the same time. It was therefore apparent that the higher flow rate had the desired effect of forcing the gas mixture deeper into the sample space. The bulk samples produced in this manner were somewhat cloudy but were nevertheless considered usable for light scattering purposes. The samples were confirmed to be methane hydrate using the test described under Method 1.

### Method 3

Since the hydrate seemed to favor growing along the cell walls, probably because it was the coldest region first encountered by the

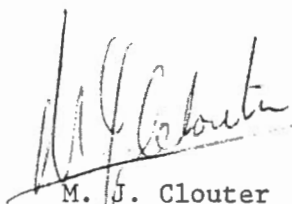
gas mixture, it was decided to introduce a cold point on the centre axis of the cell by inserting a 1 mm, pointed copper rod into the cell. The copper point was to be situated about 1 mm below the tip of the hypodermic tube and thus provide a nucleation site for the hydrate. Unfortunately (at the time of writing this report), the cell was cracked in the modification procedure. When appropriate repairs are accomplished the testing of this method will be completed.

#### PROPOSED MODIFICATIONS AND CONCLUSIONS

Even though the hydrate formation problem is a difficult one, we are optimistic that relatively clear samples can be produced, and that they will be suitable for Brillouin scattering experiments. Unless the results of Method 3 prove disappointing, the following modifications will be carried out. (1) The inner diameter of the cell will be increased to 1.5 mm and will include the bottom quartz window. (2) The size of the hypodermic tube will be decreased to 0.5 mm outer diameter and it will be adjustable in vertical position so that the end of the tube can be kept very close ( $\sim 0.5$  mm) to the hydrate nucleation surface at all times. In other words, this will ensure that the gas mixture first encounters the coldest horizontal surface rather than the cell walls. (3) By positioning the bottom clip below the top surface of the quartz window, and by adjusting the hypodermic appropriately, it should be possible to initiate hydrate growth on the surface of the window.

On the basis of the encouraging results so far obtained it is estimated that suitable samples will be available for Brillouin studies within 2 months. Brillouin scattering data should be forthcoming by the end of March 1980, and at least mean values for the speeds of longitudinal and transverse sound will be derivable from these data.

Memorial University,  
Department of Physics,  
December 8, 1979.

  
M. J. Clouter

  
H. Kiefte

## REFERENCES

- S. F. Ahmad, H. Kiefte, and M. J. Clouter 1978 J. Chem. Phys. 69, 5468-5472.
- L. Brillouin 1914 Compt. Rend. 158, 1331  
 ----- 1917 Ann. Phys. (Paris) 17, 88
- D. W. Davidson 1973 in *Water, a Comprehensive Treatise*, Vol. 2, F. Franks editor, Plenum Press, New York, pp. 115-234; 1979 private communication.
- P. H. Gammon, H. Kiefte, and M. J. Clouter 1979 J. Chem. Phys. 70, 810-815.  
 ----- 1980 J. Glaciology, in press.
- J. H. Hand, D. L. Katz, and V. K. Verma 1974 in *Marine Science*, Vol. 3, I. R. Kaplan editor, Plenum Press, New York, pp. 179-194
- H. Kiefte and M. J. Clouter 1975 J. Chem. Phys. 62, 4780-4786.  
 ----- 1976 J. Chem. Phys. 64, 1816-1819.
- Yu. F. Makogan and G. A. Sarkis'yants 1976 in *Prevention of Hydrate Formation in the Extraction and Transport of Gas*, D. W. Davidson editor, NRCC Technical Translation No. 15476.
- S. L. Miller 1974 in *Marine Science*, Vol. 3, I. R. Kaplan editor, Plenum Press, New York, pp. 151-177.
- B. P. Stoicheff 1977 in *Rare Gas Solids*, Vol. 2, M. L. Klein and J. A. Venables editors, Academic Press, New York, pp. 979-1020.
- R. D. Stoll 1974 in *Marine Science*, Vol. 3, I. R. Kaplan editor, Plenum Press, New York, pp. 235-248.
- R. D. Stoll, J. Ewing, and G. M. Bryan 1971 J. Geophys. Res. 76, 2090-2094.
- E. Whalley 1979 NRCC report and private communication.

## FIGURE CAPTIONS

- Fig. 1 (a). The Brillouin scattering mechanism; Bragg reflection of monochromatic incident radiation from an acoustic plane wave gives rise to a Doppler shift in the frequency of the scattered (reflected) radiation.
- (b). Typical Brillouin spectrum of a liquid.
- Fig. 2 Overall arrangement of the apparatus in a Brillouin scattering experiment: L, lenses; M, mirror; A, aperture; COL, x-ray collimator; S, sample site; P, Polaroid x-ray camera; PM, photomultiplier tube; AD, amplifier-discriminator; DAS, data acquisition and control system.
- Fig. 3 Schematic drawing of the cryostat.
- Fig. 4 The high pressure gas handling system.

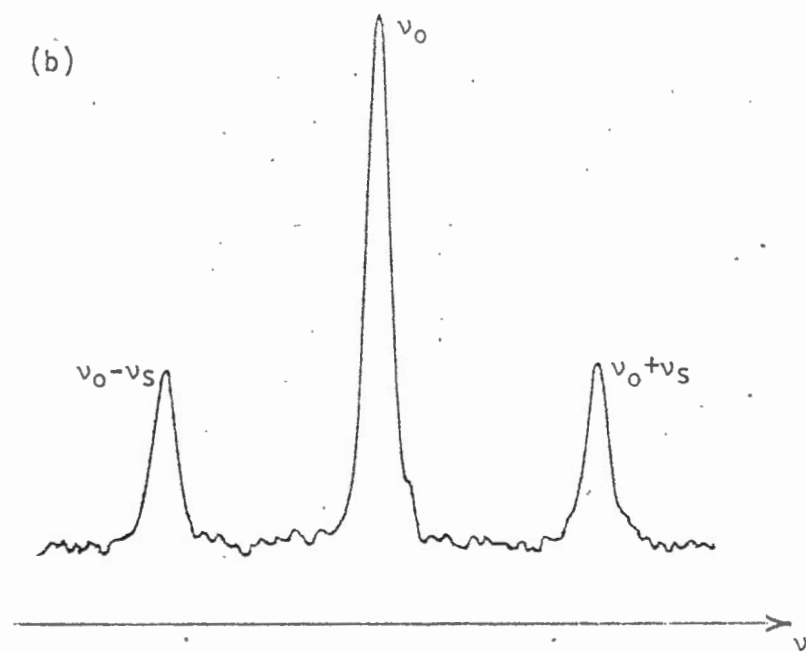
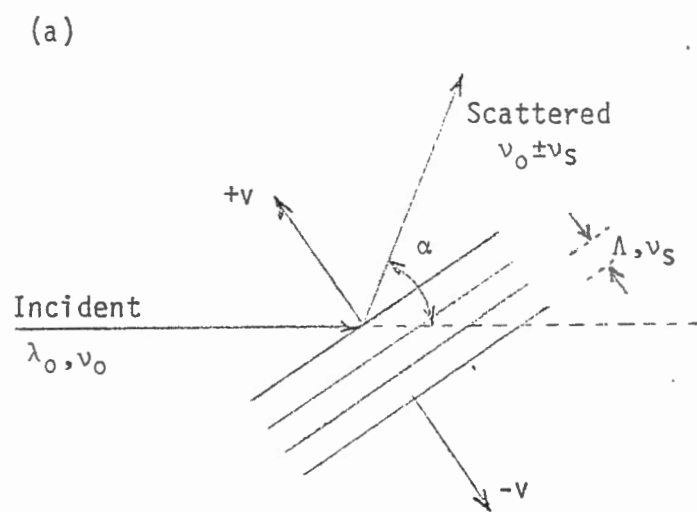


FIGURE 1

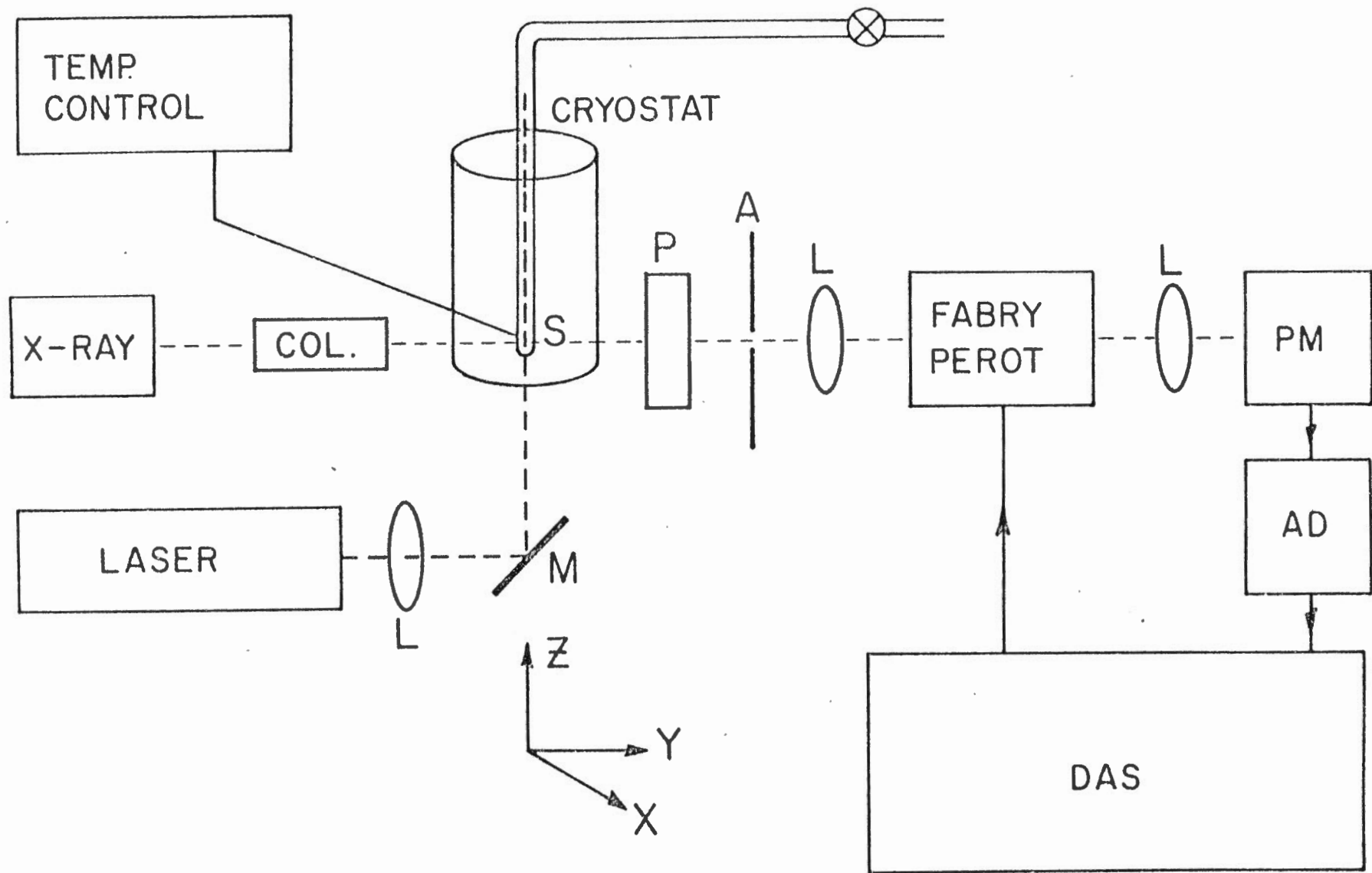


FIGURE 2



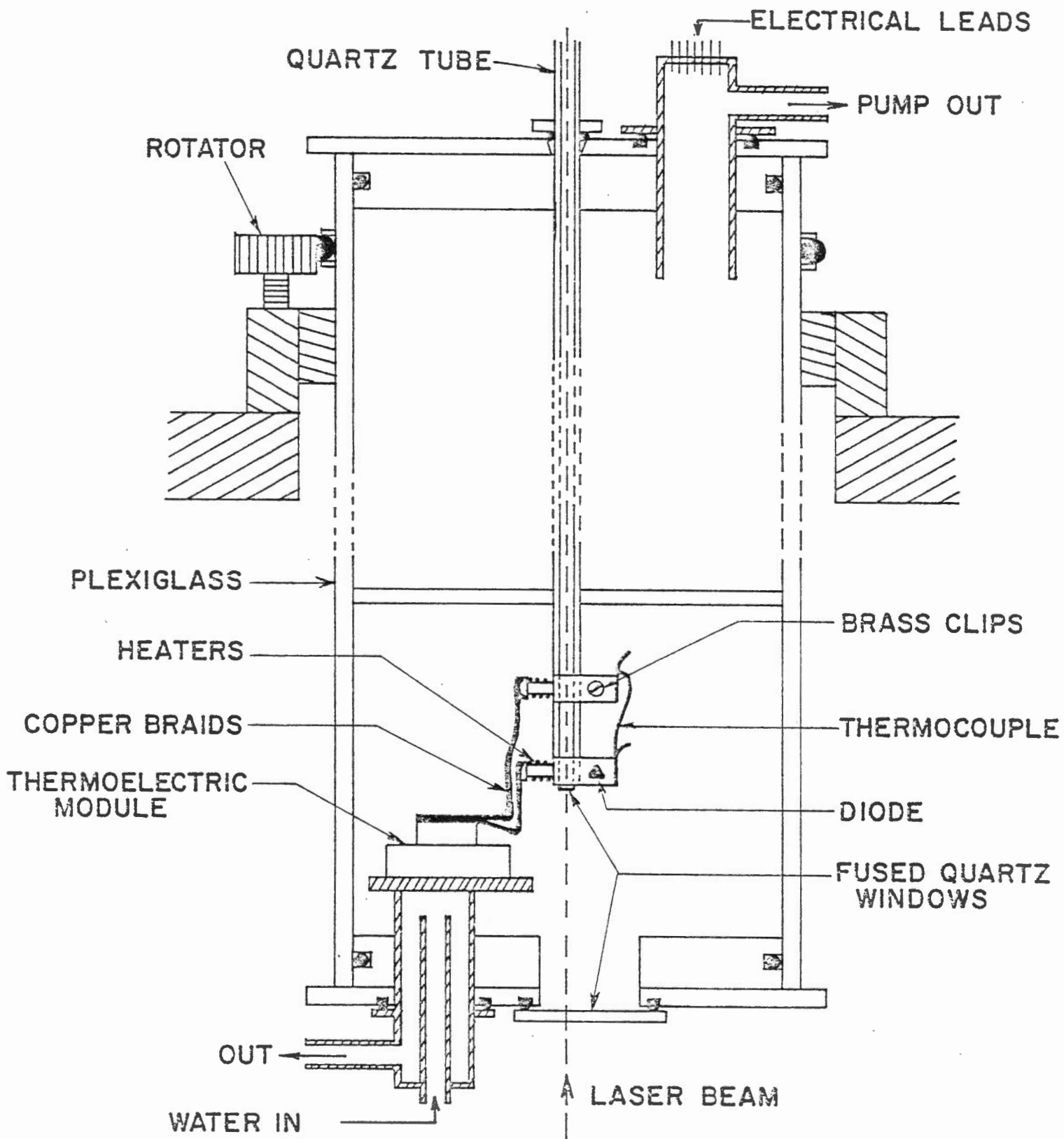


FIGURE 3

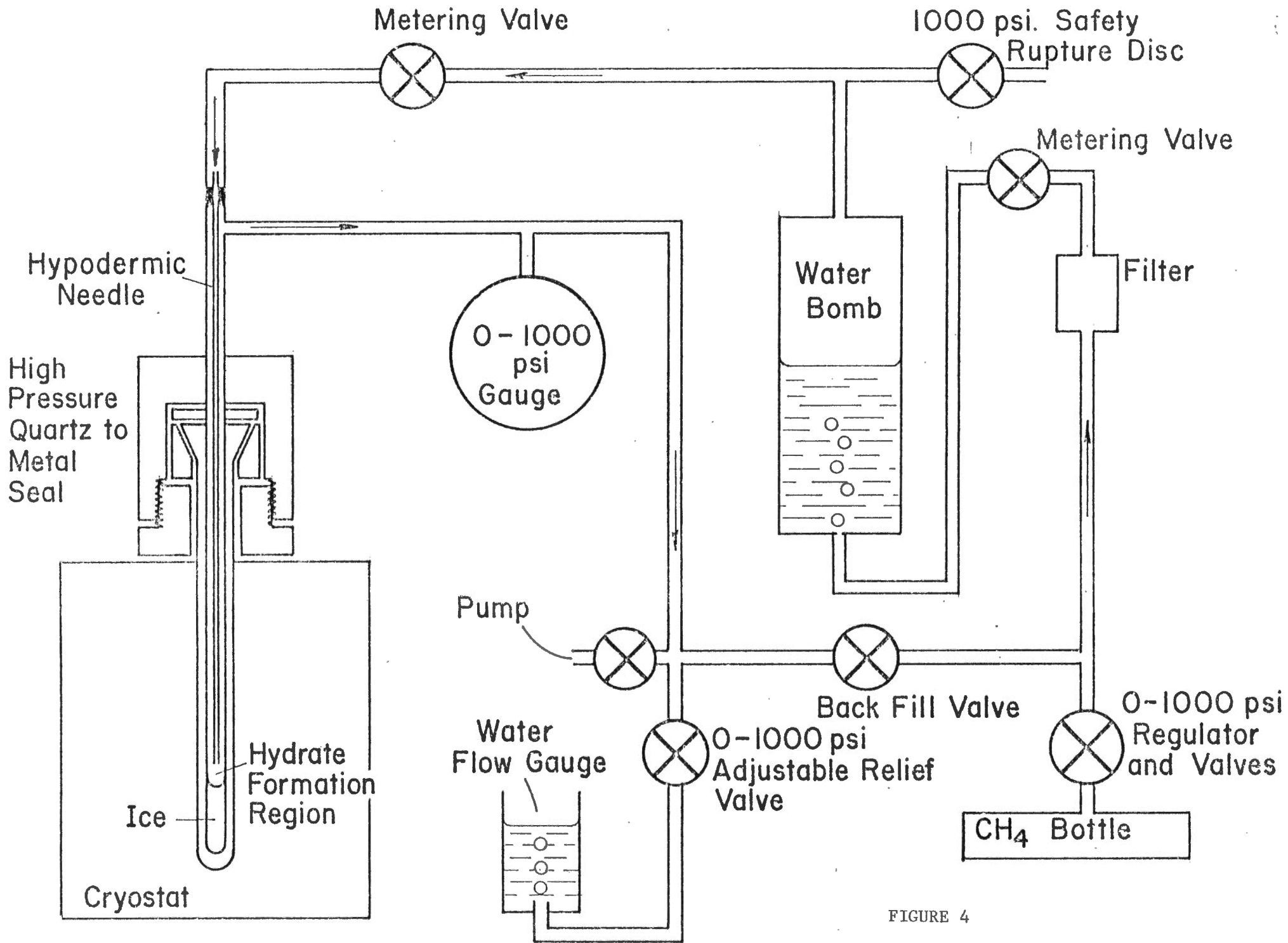


FIGURE 4